Characterization of Ligands of a High-Affinity Metal-Binding Site in the Latent Chloroplast F_1-ATPase by EPR Spectroscopy of Bound VO^{2+} †

Andrew L. P. Houseman,‡ Lola Morgan,§ Russell LoBrutto, and Wayne D. Frasch*

The Center for the Study of Early Events in Photosynthesis, Department of Botany, Arizona State University, Tempe, Arizona 85287-1601

Received December 10, 1993; Revised Manuscript Received February 23, 1994®

ABSTRACT: Vanadyl, $(V{=}O)^{2+}$, is able to substitute for Mg^{2+} as a cofactor for ATPase activity catalyzed by the chloroplast F_1-ATPase (CF_1). Mg^{2+}-dependent ATPase activity was also observed with CF_1 that contained VO^{2+}-ATP bound specifically to the noncatalytic N2 site. Modulation of the Mg^{2+}-ATPase activity induced by VO^{2+} bound at this site indicates that the metal bound to the noncatalytic site affects catalytic activity. When CF_1 is depleted of nucleotides from all but the N1 site, a single Mg^{2+} remains bound at a site designated M1. Addition of VO^{2+} to the depleted protein gives rise to an EPR spectrum characteristic of a CF_1-bound VO^{2+} species. The binding curve of the VO^{2+} complex to latent, nucleotide-depleted CF_1 was determined by the integrated intensities of the $-5/2_{\parallel}$ peak in the EPR spectrum as calibrated using atomic absorption spectroscopy. Under these conditions, VO^{2+} binds cooperatively to approximately two sites designated M2 and M3. Three-pulse ESEEM spectra of the CF_1–VO^{2+} complex contain two intense modulations with frequencies and field-dependent behavior that show that they are from a directly coordinated ^{14}N nucleus. Analysis of the bound VO^{2+} by ENDOR spectroscopy revealed the presence of a single group of protons associated with an equatorial amino or water ligand that is exchangeable with solvent. Using the additivity relation for hyperfine coupling, the most probable set of equatorial ligands to the VO^{2+} bound to CF_1 under these conditions consists of one lysine nitrogen, two carboxyl oxygens from aspartate or glutamate, and one water.

The F_1-ATPases from mitochondria, bacteria, and chloroplasts have six nucleotide-binding sites, three of which are believed to be directly involved with the ATP synthesis/hydrolysis reaction (Cross & Nalin, 1982; Xue et al., 1987; Girault et al., 1988). In the chloroplast enzyme (CF_1),[1] the six nucleotide sites fill in a specific order (N1–N6) due to decreasing binding affinities and characteristics that make each unique (Bruist & Hammes, 1981; Shapiro et al., 1991). The N1 is a catalytic site with such high affinity that nucleotide can only be removed by irreversible denaturation of the protein. The N2 is a metal-dependent, noncatalytic, nucleotide-binding site that is specific for ATP. Depleting the enzyme of metal–nucleotide from this site requires that the protein incubate for 50+ h as an ammonium sulfate precipitate in the presence of EDTA, followed by extensive gel-filtration chromatography. The other catalytic sites are believed to be N3 and N4, while N5 and N6 are weakly binding noncatalytic sites (Bruist & Hammes, 1981; Leckband & Hammes, 1987; Shapiro et al., 1991). The nucleotide in these sites can be distinguished by gel-filtration chromatography and/or equilibrium dialysis.

Divalent cations such as Mg^{2+}, Mn^{2+}, and Ca^{2+}, long known to serve as cofactors of the F_1-ATP synthesis and hydrolysis reactions, function at the catalytic sites by coordinating the phosphate oxygens of the nucleotides (Frasch & Selman, 1982; Carmeli et al., 1986). Recent studies have shown that metal-dependent nucleotide binding to the noncatalytic sites also affects the rate of catalysis (Murataliev, 1992; Jault & Allison, 1993). A total of six metal sites has been estimated to exist on the enzyme (Hochman & Carmeli, 1985). CF_1 depleted of metal nucleotides by ammonium sulfate precipitation binds divalent metals with high affinity to about two sites in a cooperative manner in the absence of nucleotides (Haddy et al., 1985; Hochman & Carmeli, 1985). However, little is understood about the amino acid side chains of the F_1-ATPase responsible for binding the metals.

The vanadyl cation has been used as a probe of the ligands that compose the Mg^{2+}-, Ca^{2+}-, and Mn^{2+}-binding sites of several proteins, including carboxypeptidase (DeKoch et al., 1974), *S*-adenosylmethionine synthetase (Markham et al., 1984; Zhang et al., 1993), and pyruvate kinase (Tipton et al., 1989; Lord & Reed, 1990), among others (Eaton & Eaton, 1990). Vanadyl is a cation composed of vanadium(IV) double-bonded to oxygen to give a net charge of 2+. This cation specifically binds to the divalent cation-binding sites of several enzymes, including sites composed of metal–nucleotide complexes, and in many cases VO^{2+} serves as a functional cofactor (Eaton & Eaton, 1990). Vanadyl has one axial and four equatorial coordination sites relative to the axis of the double-bonded oxygen. Since ^{51}V has a nuclear spin $I = {}^7/_2$, its nuclear hyperfine coupling can serve as a sensitive probe of the coordination chemistry of protein metal-binding sites

† This work was supported in part by grants from the H. Frasch Foundation (0188HF) and a U.S. Department of Agriculture NRIC grant (92-01249) to W.D.F. Support was also provided by a grant from the Howard Hughes Medical Institute through the Undergraduate Biological Sciences Education Program. This is publication no. 187 of the Center for the Study of Early Events in Photosynthesis. The Center is supported by U.S. Department of Energy Grant DE-FG02-88ER13969.

* Author to whom correspondence should be addressed.

‡ ASU Center for the Study of Early Events in Photosynthesis Postdoctoral Research Fellow.

§ Howard Hughes Medical Institute Research Fellow.

® Abstract published in *Advance ACS Abstracts,* April 1, 1994.

[1] Abbreviations: AdoMet, *S*-adenosylmethionine; CF_1, soluble chloroplast F_1-ATPase; cw-EPR, continuous wave electron paramagnetic resonance spectroscopy; ESEEM, electron spin–echo envelope modulation spectroscopy; ENDOR, electron–nuclear double resonance spectroscopy; HEPES, *N*-(2-hydroxyethyl)piperazine-*N*′-2-ethanesulfonic acid; N1, nondissociable catalytic nucleotide binding site; N2, metal–ATP-specific site dissociable only upon precipitation in $(NH_4)_2SO_4$ and EDTA; N3, most tightly bound ADP-specific dissociable catalytic site; PPP_i, triphosphate.

0006-2960/94/0433-4910$04.50/0 © 1994 American Chemical Society

using EPR. The small g anisotropy of VO^{2+} sometimes allows the resolution of superhyperfine couplings from ligated nuclei, leading to the identification and characterization of ligands, including the discrimination of axial versus equatorial ligands.

We now present an initial characterization of the binding of VO^{2+} to latent soluble CF_1 from spinach. In these studies, CF_1 was depleted of metals and nucleotides as per Bruist and Hammes (1981). The depleted enzyme contained a single Mg^{2+} bound at what we now define as the M1 site. The cooperatively binding high-affinity sites, now designated M2 and M3, were then filled with VO^{2+}. Using VO^{2+} as a paramagnetic probe, analyses by cw-EPR, ENDOR, and ESEEM are consistent with the presence of one water oxygen that is exchangeable with solvent, two carboxyl oxygens from either aspartate or glutamate side chains, and a single nitrogen, possibly from a lysine, comprising the equatorial ligands of the metal at this site.

EXPERIMENTAL PROCEDURES

Protein Purification and Preparation of Nucleotide-Depleted CF_1. Chloroplast F_1 was solubilized and purified from spinach thylakoids as per Frasch and Selman (1982). The enzyme was depleted of metal nucleotides from all but the N1 metal–nucleotide site, as per Bruist and Hammes (1981), by storage as a precipitate in a 50% saturated solution of ammonium sulfate that contained 2 mM EDTA and 25 mM Tris-HCl (pH 8.0). The protein was resuspended in 2 mM EDTA/50 mM HEPES (pH 8.0) buffer and desalted over a 50 × 2.5 cm Sephadex G-50-80 chromatography column equilibrated with the same buffer. After elution from the column, the protein was concentrated by pressure dialysis and chromatographed on a second 50 × 2.5 cm Sephadex G-50-80 column equilibrated in 50 mM HEPES at pH 8.0. The protein was then concentrated to 0.25–0.4 mL, rapidly frozen in liquid nitrogen, and stored in liquid nitrogen until use. In some samples, the second chromatography column was equilibrated in 50 mM HEPES (pH 8.0) dissolved in D_2O (>90%). The protein that eluted from the column was concentrated to 0.4 mL, diluted in 99+% D_2O, and then concentrated and frozen as before. Protein concentration was determined by the extinction coefficient at 277 nm as per Bruist and Hammes (1981) using a molecular weight of 410 000 (Moroney et al., 1983).

EPR, ENDOR, and ESEEM Measurements. cw-EPR experiments were carried out at X-band (9 GHz) using a Bruker 300E spectrometer and a liquid nitrogen flow cryostat operating at 100 K. Simulations of the cw-EPR spectra employed the program QPOWA (Nilges, 1979; Maurice, 1980), which was the generous gift of J. Telser. This program employs the equation taken from Froncisz and Hyde (1980) to describe line widths as a function of the magnetic quantum number, m_I. The line widths are composed of the residual line widths, W, the A-strain parameter, C_1, the g-strain parameter, C_2, and the constant ϵ which correlates C_1 and C_2.

cw-ENDOR measurements employed the same spectrometer and the Bruker low-temperature ENDOR accessory, which incorporates an Oxford Model 900 liquid helium flow cryostat. ENDOR was employed to measure ^1H superhyperfine couplings to VO^{2+}. The first-order ENDOR transition frequencies $\nu_\pm$ for $I = {}^1/_2$ nuclei are given by

$$\nu_\pm = |\nu_L \pm A/2| \quad (1)$$

where A is the orientation-dependent hyperfine coupling constant, and ν_L is the Larmor frequency of the resonant nucleus (Abragam & Bleaney, 1970).

ESEEM was used to detect ^{14}N superhyperfine couplings to VO^{2+}. Three-pulse (stimulated echo) ESEEM experiments were carried out at 4–5 K using a lab-built spectrometer (LoBrutto et al., 1986) operating over the 7–11-GHz range and an APD Cryogenics LTR flow cryostat. In cases where the isotropic part of the superhyperfine coupling, A_{iso}, is large relative to the nuclear Zeeman and nuclear quadrupole interactions, two very sharp "double quantum" ($\Delta m_I = \pm 2$) nuclear transitions generally are observed at frequencies given by

$$\nu_\pm = 2[(\nu_L \pm A_{iso}/2)^2 + K^2(3 + \eta^2)]^{1/2} \quad (2)$$

where K and η are parameters that describe the nuclear quadrupole coupling (Astashkin & Dikanov, 1985). A very good approximation of A_{iso} can be obtained (Reijerse et al., 1989) by rearranging eq 2:

$$A_{iso} = (\nu_+^2 - \nu_-^2)/8\nu_L \quad (3)$$

The value of A_{iso} was used in the present study to characterize the residue donating a ligand to VO^{2+}.

Time domain ESEEM spectra were truncated to remove instrumental dead time at the beginning of the data record. The deleted section was set to zero, and the remainder of the spectrum was apodized to reduce artifacts in the Fourier transform. The time domain data record was then zero-filled to 2048 points and Fourier transformed. ESEEM spectra are displayed in the frequency domain as power spectra.

Correlation of EPR Signal Intensities and VO^{2+} Concentration. VO^{2+}–ATP was added to metal–nucleotide-depleted CF_1, which was then chromatographed on a 50 × 2.5 cm Sephadex G-50-80 column equilibrated with 50 mM HEPES buffer (pH 8.0) to remove all VO^{2+} not tightly bound. The $-{}^5/_{2\|}$ EPR signal of bound VO^{2+} was integrated and then correlated to the abundance of vanadium by atomic absorption spectroscopy using a Shimadzu 670G spectrometer with a graphite furnace. The uncertainty in the conversion from signal area to concentration is ±10%.

Preparation of VO^{2+} Solutions. Vanadyl was added in stoichiometric amounts to latent, metal–nucleotide-depleted CF_1 using a solution of freshly prepared $VOSO_4$, from which dissolved molecular oxygen had been removed by purging with dry nitrogen gas. In some samples, VO^{2+} was stabilized in solution by rapidly adding $VOSO_4$ with vigorous stirring to a solution of ATP at pH 6.0 that had been degassed with dry nitrogen. Solutions that contain a mole ratio of ATP:VO^{2+} as low as 0.7:1.0 are stable for a period of 24 h at room temperature under these conditions.

ATPase Assays. The rate of ATP hydrolysis was measured as discontinuous assays of phosphate formation (Chen et al., 1956) of 5 min duration in a reaction mixture that contained 30 mM tricine (pH 8.0) and the concentrations of ATP and Mg^{2+}, Ca^{2+}, or VO^{2+} indicated. Assays contained 3 μg of CF_1 as determined by the Bradford assay, which was activated by 50 mM dithiothreitol and 3% ethanol that was present in the reaction mixture.

RESULTS

CF_1 Catalyzes VO^{2+}-Dependent ATP Hydrolysis. The steady-state rates of ATP hydrolysis catalyzed by CF_1 as a function of Ca^{2+}-ATP, Mg^{2+}-ATP, or VO^{2+}-ATP concentration are shown in Figure 1. The VO^{2+}-ATPase was sustained

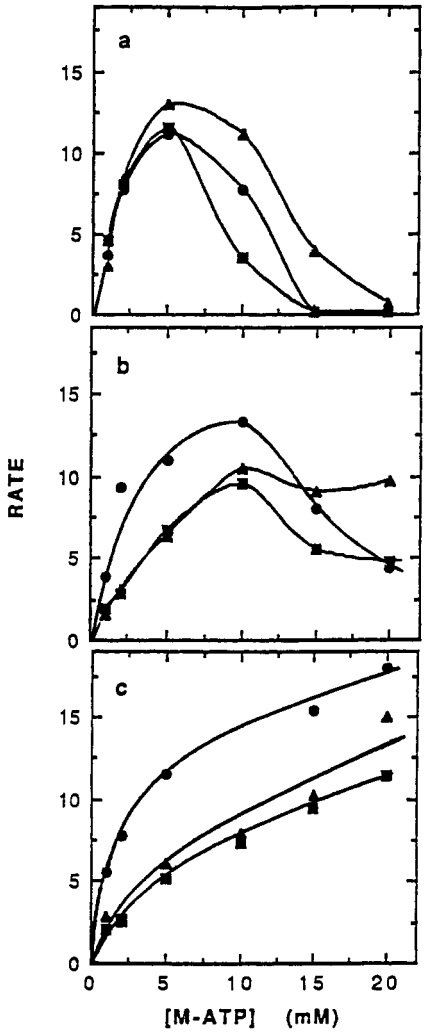

FIGURE 1: Comparison of Mg^{2+}-dependent (■), Ca^{2+}-dependent (●) and VO^{2+}-dependent (▲) ATPase activity of CF_1 as a function of the concentration of the metal–ATP complex. The mole ratio of metal:ATP was maintained at 0.5:1 (a), 1:1 (b), and 1.5:1 (c). The CF_1 used in these assays was depleted of metal–nucleotides from all but the N1 site prior to assay. The rate of ATPase activity is expressed as μmol of ATP/(mg of CF_1)·min.

for more than 20 min (data not shown). Both free metal and free ATP in solution are known to inhibit the rate of ATPase activity of CF_1 (Hochman & Carmeli, 1981). The data of Figure 1a–c compare the effectiveness of the three cations serving as cofactors for the ATPase reaction under conditions in which the metal:ATP ratio was maintained at 0.5:1, 1:1, and 1.5:1, respectively. When the metal was in excess such that the amount of free ATP was minimized (Figure 1c), the ATPase activity showed a hyperbolic dependence versus the metal–ATP concentration. When CF_1 was activated by the addition of dithiothreitol and ethanol to the assay mixture, the apparent V_m of VO^{2+} was more comparable to that of Ca^{2+} than to Mg^{2+} (20, 22, and 13 μmol of ATP/(mg of CF_1)·min, respectively). However, the V_m/K_M values of VO^{2+} and Mg^{2+} were significantly lower than that of Ca^{2+} (2.4, 1.7, and 8.8, respectively). Vanadyl is unstable in aqueous solution at pH 8.0 in the absence of a chelator and will precipitate out of solution as $[VO(OH)_2]_n(s)$. The rate of precipitation depends on the relative abundance and affinity of the chelator. Since maximum stability is obtained at metal:ATP ratios of 0.5:1 (Mustafi et al., 1992), the data in Figure 1c probably do not reflect the actual concentration of VO^{2+} in solution, and hence the concentration of VO^{2+}-ATP in solution is

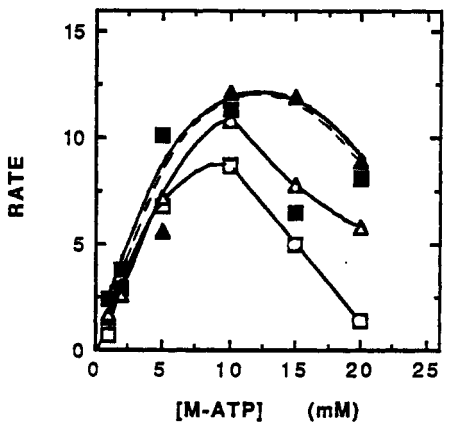

FIGURE 2: Effect of preloading the N2 site with ATP and Mg^{2+} (closed symbols) or VO^{2+} (open symbols) on the rate of Mg^{2+}-dependent (squares) and VO^{2+}-dependent (triangles) ATPase activity as a function of the concentration of the metal–ATP complex. In all assays, the mole ratio of metal:ATP was 1:1. The rate of ATPase activity is expressed as μmol of ATP/(mg of CF_1)·min.

probably somewhat lower than that shown. Thus, the effective V_m/K_M may be closer to that of Ca^{2+} than is apparent from these data.

When the metal:ATP ratio was maintained at 0.5:1 (Figure 1a), the inhibition by free ATP was clearly evident at free ATP concentrations 5 mM and above, regardless of the metal used. The ATPase activity was inhibited to a somewhat smaller extent with VO^{2+} present than with Mg^{2+} or Ca^{2+}. At a 1:1 metal:ATP ratio (Figure 1b), the inhibition by free ATP at higher substrate concentrations is visible. The concentration of metal–ATP that gives rise to the highest ATPase rate is also shifted from 5 to 10 mM when the metal:ATP ratio is changed from 0.5:1 to 1:1, suggesting that the inhibition induced by free metal primarily affects the V_m/K_M of the reaction. Consistent with the data of Figure 1c, the inhibition induced by free VO^{2+} is comparable to that of free Mg^{2+}.

The noncatalytic N2 site specifically binds metal–ATP, which can only be removed by a 50+ h incubation in EDTA as a protein precipitate in ammonium sulfate followed by extensive gel-filtration chromatography (Bruist & Hammes, 1981). The effects of preloading the noncatalytic N2 site of CF_1 with VO^{2+}-ATP or Mg^{2+}-ATP on the ATPase activity were examined by depleting the latent enzyme of nucleotides from the N2–N6 sites (see Experimental Procedures), filling the N2 site with metal–ATP, and then removing metal–ATP from sites other than N2 via chromatography on Sephadex G-50-80 prior to activation and assay.

As shown in Figure 2, CF_1 that contained Mg^{2+}-ATP at N2 exhibited about the same kinetics of ATPase activity using a 1:1 metal:ATP ratio for substrate as when the site had not been specifically filled prior to assay (Figure 1b). There were also no dramatic differences in the substrate dependence of ATPase activity when the N2 site had been preloaded with VO^{2+}-ATP. The only differences were found at the higher substrate concentrations where, as suggested by Figure 1, inhibition by free ATP becomes significant. At these substrate concentrations, the Mg^{2+}-dependent rate of the CF_1 preloaded with VO^{2+}-ATP at N2 was inhibited to the greatest extent, while the VO^{2+}-dependent rate of the preloaded Mg^{2+}-ATP enzyme was inhibited the least.

Quantitation of Metal Binding to Nucleotide-Depleted CF_1. The abundance of Mg, Mn, and V bound to CF_1 was determined by atomic absorption spectroscopy after treatments known to fill or deplete CF_1 of metals and nucleotides at specific

Table 1: Metal Content of CF_1 As Determined by Atomic Absorption Spectroscopy

treatment	mole ratio metal:CF_1[a]	
	Mg	V
$ndCF_1$[b]	0.96 ± 0.11	0.00
$ndCF_1$ + VO^{2+}-ATP at N2[c]	1.00 ± 0.10	0.44 ± 0.12
$ndCF_1$ + VO^{2+}-ATP at N2 then nd[d]	0.83 ± 0.18	<0.05

[a] Average of at least three determinations from each of 2–5 samples. [b] Nucleotide-depleted CF_1 by ammonium sulfate precipitation (Experimental Procedures); contains only ADP at N1. [c] After the addition of 3 mol equiv of VO^{2+}-ATP followed by Sephadex G-50-80 chromatography to deplete metal–nucleotides (Experimental Procedures). [d] Sample with VO^{2+}-ATP at N2 was then depleted of metal and ATP from N2 by ammonium sulfate precipitation.

sites. The standard treatment used here to deplete CF_1 of dissociable metals and nucleotides employs a 50+ h incubation as an ammonium sulfate precipitate with EDTA followed by extensive gel filtration (Bruist & Hammes, 1982; Haddy et al., 1985). As shown in Table 1 (row 1), the enzyme still contains about one Mg after this treatment, which we now define as bound to the M1 site. This agrees with previous determinations under similar conditions (Hiller & Carmeli, 1985; Haddy et al., 1989). Approximately one tightly bound ADP at the N1 site also survives this treatment (Bruist & Hammes, 1982). The N2 site, which is specific for ATP and dependent on the metal for binding, can be filled after this depletion treatment.

Table 1 (row 2) shows the abundance of metals bound to metal–nucleotide-depleted CF_1 after the addition of a single equivalent of VO^{2+}-ATP followed by gel-filtration chromatography, which is known to remove nucleotides from all but the N1 and N2 sites (see Experimental Procedures). The enzyme treated in this manner still contains the single tightly bound Mg at M1 as well as 0.44 equiv of vanadium, which we define as bound to the M2 site. The purified enzyme contained relatively little bound Mn (data not shown), even though Mn is available in chloroplasts. The ammonium sulfate precipitation method, known to deplete ATP from the N2 site, also removed the V bound to the M2 site of the samples of Table 1 (row 2) as shown in row 3. Thus, the binding properties of the M2 metal site correlate with the N2 nucleotide site. The amount of Mg bound to the M1 site remained largely unaffected by the second ammonium sulfate precipitation.

Characterization of Bound VO^{2+} by cw-EPR. The cw-EPR spectrum of VO^{2+} bound to CF_1 is shown in Figure 3a. This spectrum exhibits large ^{51}V hyperfine splittings from molecules with the V=O bond oriented along the magnetic field ($A_\parallel$) and small hyperfine splittings from molecules with the V=O bond perpendicular to the magnetic field ($A_\perp$). Each of the eight widely spaced resonances roughly separated by $A_\parallel$ arises from an electronic transition between the $m_s = \pm 1/2$ states, but with different, unchanging nuclear spin states: $m_I = \pm 7/2, \pm 5/2, \pm 3/2$, and $\pm 1/2$. The same is true for the more intense, narrowly spaced resonances roughly separated by $A_\perp$. Thus, each feature can be designated according to its m_I. These spin-Hamiltonian parameters of the spectrum of Figure 3a are given in Table 2 as derived by simulation using the QPOWA program. The simulated spectrum using these couplings is shown in Figure 3b.

The $-5/2_\parallel$ peak (Figure 3a, feature A) is the most intense peak in the EPR spectrum that contains contributions from $A_\parallel$ but not from $A_\perp$. Weil and Hecht (1963) have demonstrated that the $-5/2_\parallel$ signal is a true absorption signal under the conditions used in the EPR experiments, so that the integrated intensity of this feature is directly proportional to

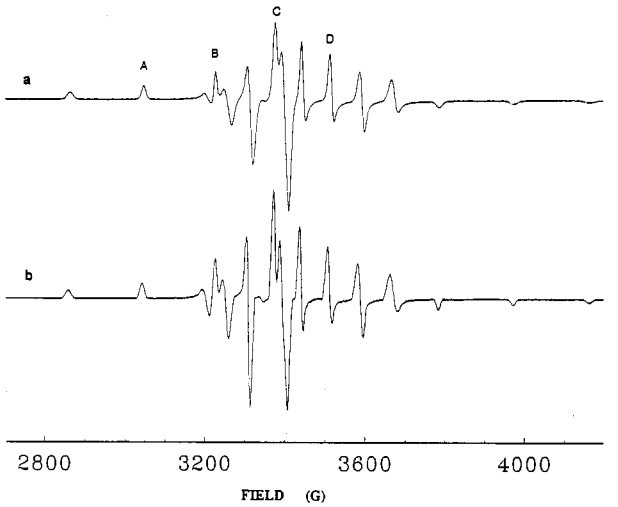

FIGURE 3: (a) Continuous wave EPR spectrum of VO^{2+} bound to latent CF_1 depleted of metals and nucleotides from all but the N1 site. Conditions include the following: field modulation frequency, 100 kHz; modulation amplitude, 0.50 mT; sweep rate, 0.95 mT/s; time constant, 82 ms; microwave frequency, 9.5556 GHz; microwave power, 1.0 mW; temperature, 101 K. (b) Simulated spectrum of the bound VO^{2+} using the QPOWA program with the spin-Hamiltonian parameters shown in row 1 of Table 2 and the line-width parameters W = [16, 16, 14] G, C_1 = [6.5, 6.5, 5.0] G, $C_2 = 0$, and $\epsilon = 0$.

the concentration of the VO^{2+} species in resonance. Thus, comparison of the $-5/2_\parallel$ signal from a sample of unknown concentration with the signal from a sample of known concentration provides a measure of the concentration in the unknown sample. The $-5/2_\parallel$ peak of Figure 3a can be described by a single Gaussian line shape centered at 3037 G with a half-width at half-height of 5.5 G.

Figure 4 shows the extent of binding of VO^{2+} to metal–nucleotide-depleted CF_1 as a function of added VO^{2+}. The amount of bound VO^{2+} was determined by the area under the $-5/2_\parallel$ peak of the EPR signal that arises from VO^{2+} bound to CF_1. The relationship between the integrated area of this peak and the abundance of bound VO^{2+} was established using samples of VO^{2+} bound to CF_1 in which VO^{2+} in solution had been removed by chromatography (Table 1, row 2) as described in the Experimental Procedures. Under these conditions, the protein binds approximately two VO^{2+}/CF_1, with a sigmoidal dependence on the amount of added metal characteristic of cooperative binding. The peak-to-peak amplitudes of the $-1/2_{\perp,\parallel}$ and $+3/2_\perp$ features in the EPR spectrum (Figure 3a, features C and D, respectively) that arise as a function of added VO^{2+} showed the same sigmoidal dependence (data not shown). Due to the instability of VO^{2+} in aqueous solution at pH 8.0 in the absence of a chelator, it was not possible to calculate the dissociation constant(s) and the Hill coefficient for VO^{2+} binding under these conditions. However, similar high-affinity cooperative binding has been observed for manganese under the same conditions (Haddy et al., 1985; Hochman & Carmeli, 1985), further indicating that VO^{2+} has bound to the functional metal-binding sites on CF_1.

VO^{2+} Bound to CF_1 Is Coordinated Equatorially by ^{14}N. The ligand environment of the VO^{2+} bound to CF_1 as described in Figure 4 was examined by electron spin–echo envelope modulation (ESEEM) spectroscopy. ESEEM can detect interactions between the electron spin of VO^{2+} ($S = 1/2$) and nuclear spins such as ^1H ($I = 1/2$), ^{31}P ($I = 1/2$), and ^{14}N ($I = 1$) if they are sufficiently close to the bound VO^{2+}. Figure 5 shows ESEEM spectra of the bound VO^{2+} at a single microwave frequency at magnetic field settings of 0.297, 0.311,

Table 2: EPR Parameters of VO^{2+} Complexes Determined Experimentally and by the Additivity Relationship

VO^{2+} equatorial ligands	A_0	^{51}V ($\times 10^{-4}$ cm^{-1}) $A_\parallel$	$A_\perp$	$g_\parallel$	$g_\perp$	reference
CF_1	5.0	169.1	60.4	1.947	1.982	this paper
AdoMet synthetase						Zhang et al., 1993; Markham, 1984
(i) 1 RNH_2 (K^a), 2 P_i (ATP), 1 H_2O?	4.3	175	67.6	1.94	1.97	
(ii) 1 RNH_2 (K^a), 2 P_i (PPP_i), 1 H_2O?	4.8	175	67.6	1.94	1.97	
(iii) 1 RNH_2 (AdoMet), RO^- ? (S or T)	5.5	164	58.0	1.95	2.00	
pyruvate kinase						Tipton et al., 1989; Lord & Reed, 1990
1 RNH_2 (K^a), 2$RCOO^-$ (pyruvate), 1 P_i	4.9	172.0	63.6	1.9032	1.971	
apoferritin, 1 R = NR′ ($H^{a,b}$), O's?	6.5					Gerfen et al., 1991
transferrin						White & Chasteen, 1979; Eaton et al., 1989
1 R=NR′ ($H^{a,b}$) 2 $RCOO^-$ (oxalate)		171.2	60.1	1.941	1.979	
carboxypeptidase						DeKoch et al., 1974
2 R=NR′ (H^a), 1 $RCOO^-$ (E^a)		165.9	61.1	1.944	1.978	
$(imidazole)_4$, 4 R=NR′	6.6[c]	162.1	57.4	1.952	1.981	Mulks et al., 1982
$(glycine)_2$, 2 RNH_2, 2 $RCOO^-$	5.0	165.0				Tipton et al., 1989; Holyk, 1979
$(NH_3)_4$, 4 RNH_2	5.6[c]					Kirste & van Willigen, 1982
$(ethylenediamine)_2$, 4 RNH_2		160.3		1.955		Holyk, 1979
$(oxalate)_2$, 4 $RCOO^-$		170.9		1.941		Holyk, 1979
$(H_2O)_4$		182.6		1.933		Albanese & Chasteen, 1978a,b
2 RNH_2, 2 H_2O		172.4		1.944		*d*
1 RNH_2, 2 $RCOO^-$, 1 H_2O		171.6		1.9525		*d*
1 RO^-, 1 $RCOO^-$, 2 H_2O		169.35		1.9435		*d*

[a] Refers to single letter abbreviation of amino acid side chain. [b] As estimated only from the ESEEM ^{14}N coupling shown. [c] A_z was used instead of A_0, but for comparison A_z = 6.5 MHz for R=NR′ ligands (Kirste & van Willigen, 1982). [d] Derived from eq 4.

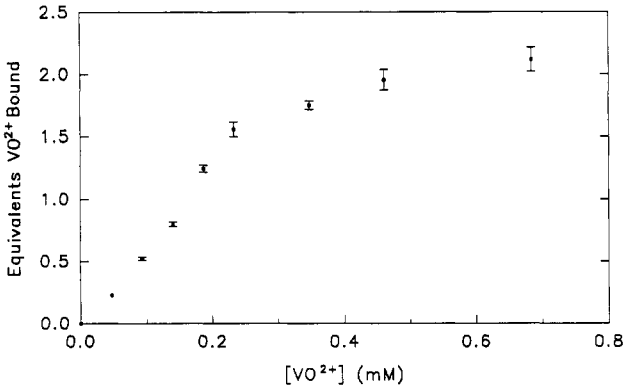

FIGURE 4: Extent of binding of VO^{2+} to latent, metal–nucleotide-depleted CF_1 as a function of added VO^{2+}. The amount of bound VO^{2+} was determined from the integrated intensity of the $-^5/_{2\parallel}$ peak of the cw-EPR spectrum (feature A, Figure 3). The extent of VO^{2+} binding was also determined from the peak-to-peak amplitudes of the $-^1/_{2\perp,\parallel}$ and $+^3/_{2\perp}$ features, respectively, in the EPR spectrum (Figure 3a, features C and D), which were included in the associated error measurement. The relationship of the intensity to the amount of bound vanadyl was determined by atomic absorption spectroscopy of bound vanadium using VO^{2+} specifically bound to the N2 site from Table 1 as described in the Experimental Procedures.

and 0.325 T, which correspond to the $-^3/_{2\parallel}$, $-^1/_{2\perp,\parallel}$, and $+^3/_{2\perp}$ features, respectively, in the EPR spectrum (Figure 3a, features B–D). Two intense nuclear transition frequencies are observed at about 4 and 7 MHz that show only small shifts in frequencies upon changing the magnetic field setting.

The positions and separation of the two resonances eliminate ^1H and ^{31}P as possible causes of the observed resonances. Since ^1H and ^{31}P have $I = ^1/_2$, only transitions of the type $\Delta m_I = \pm 1$ are possible, which would be described by eq 1. According to this equation, ^1H resonances would be centered around the ^1H Larmor frequency, ν_H = 14 MHz, which is much higher than the observed resonances. Similarly, ^{31}P modulations would either be centered at $A/2$ and split by $2\nu_P$ or centered at ν_P and split by A. The former is not possible because $2\nu_P$ is about 10 MHz, whereas the peak-to-peak separation of the observed modulations in Figure 5 is only 3 MHz, nor can the modulations be centered at ν_P because an increase in the magnetic field of about 10% from 0.297 (Figure 5a) to 0.325 T (Figure 5c) would shift the midpoint of the pair of peaks to higher frequency by an equal percentage, or 0.5 MHz. The much smaller shift of these frequencies with magnetic field observed in Figure 5 identifies these features as ^{14}N $\Delta m_I = \pm 2$ double quantum transitions (eq 2). Such transitions typically dominate the ^{14}N ESEEM spectrum when the isotropic hyperfine coupling is much larger than the nuclear Zeeman or quadrupolar interactions.

On the basis of this assignment, the isotropic superhyperfine coupling was calculated from the frequencies observed in Figure 5 using eq 3 to be 5.0 ± 0.1 MHz. A coupling this large only occurs if the ^{14}N nucleus is coordinated to VO^{2+} directly. Each of the field positions from which ESEEM was obtained contains contributions, in varying proportions, from both parallel and perpendicular orientations. The lack of variation in the coupling as observed from the $-^3/_{2\parallel}$, $-^1/_{2\perp,\parallel}$, and $+^3/_{2\perp}$ hyperfine transitions therefore suggests that it is fairly isotropic, although inadequate signal-to-noise from a purely parallel orientation (e.g., $-^5/_{2\parallel}$) prevented the determination of the dipolar part of the ^{14}N tensor. ESEEM spectra from control samples in which CF_1 was omitted from the solution revealed no ^{14}N modulations (data not shown). Therefore, the coordinated ^{14}N nucleus must result from a ligand to VO^{2+} that originates from the protein.

VO^{2+} Bound to CF_1 Has a Weak Coupling to Exchangeable Protons. Electron–nuclear double resonance (ENDOR) spectra of VO^{2+} bound to CF_1 are shown in Figure 6, centered about the proton Larmor frequency ν_H = 14 MHz. In order to distinguish exchangeable from nonexchangeable protons, spectra a and b were obtained from a sample in H_2O, whereas spectrum c was obtained from a sample in D_2O, as described in the Experimental Procedures. Spectra a–c were taken at the $-^5/_{2\parallel}$, $-^3/_{2\parallel}$, and $-^3/_{2\parallel}$ features of the cw-EPR spectrum (Figure 3a, features A and B), respectively.

When H_2O was used as the solvent, the ^1H ENDOR signal arising from the bound VO^{2+} shows a $\nu_\pm$ doublet with a weak coupling of $|A_{zz}|$ = 2.2 MHz. This weakly coupled proton is absent from the ENDOR spectrum of the VO^{2+} bound to CF_1 that had been thoroughly exchanged in D_2O, indicating that the coupling originated from an exchangeable proton(s). One water ligand has been observed coordinated to Mn^{2+} bound

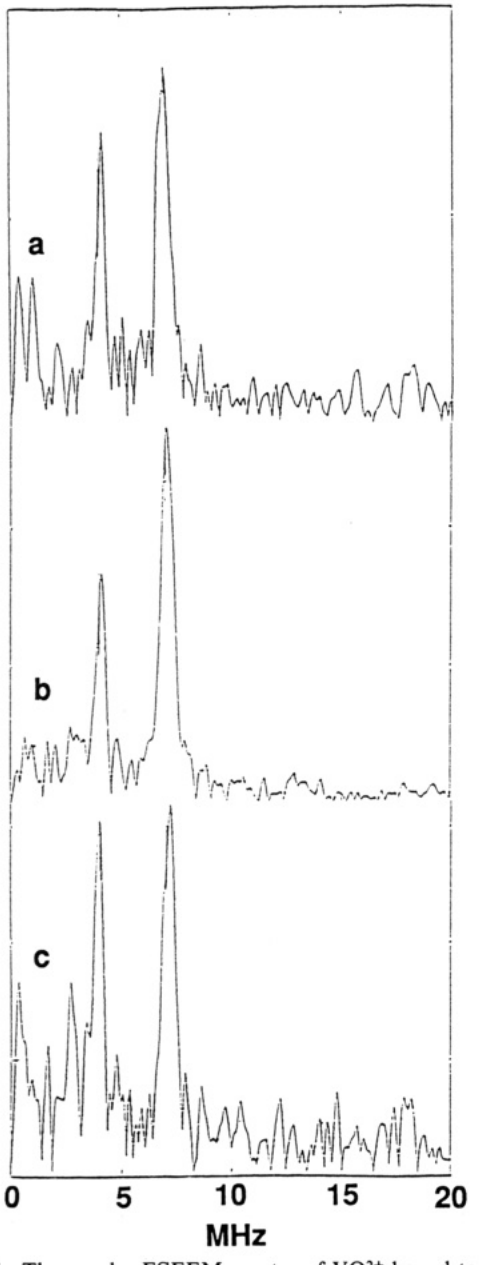

FIGURE 5: Three-pulse ESEEM spectra of VO^{2+} bound to latent, metal–nucleotide-depleted CF_1 obtained at the following field settings: (a) 0.297 T; (b) 0.311 T; and (c) 0.325 T. Other conditions include the following: frequency, 8.8711 GHz; pulse repetition rate, 100 Hz; τ, 160 ns; data points, 1024; step size, 10 ns. Each point is an average of 96 total repetitions.

to CF_1 under approximately the same conditions (Haddy et al., 1989), and we have observed a nitrogen ligand to the VO^{2+}. Since the hyperfine tensors for water and amine nitrogen are nearly identical, the proton(s) that gives rise to the 2.2-MHz coupling may arise from either or both of these groups.

The ENDOR spectra of Figure 6 provide enough information to determine whether the ligand that gives rise to the 2.2-MHz coupling is bound to the axial versus equatorial position of the metal. This is true for either a water or nitrogen ligand because of the similarity in their tensors. Water and amine groups exhibit axially symmetric superhyperfine tensors when ligated to either the equatorial or the axial position of VO^{2+} as illustrated in the inset to Figure 6 (Atherton & Shackleton 1980; Böttcher et al. 1979). For coordination to the axial VO^{2+} position, the protons should have $|A_\parallel| = 6.5$ and $|A_\perp| = 3.3$ MHz, and the tensor should be oriented with

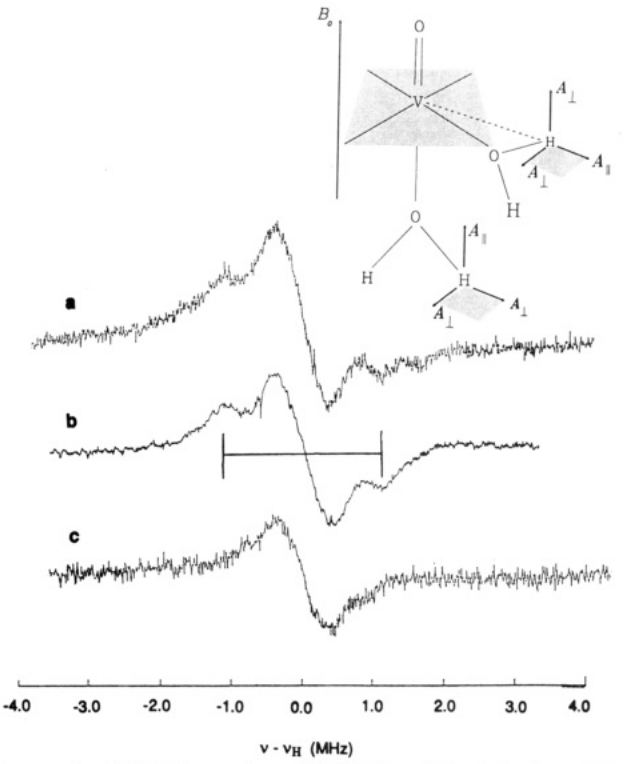

FIGURE 6: ENDOR spectra of VO^{2+} bound to latent, metal–nucleotide-depleted CF_1 obtained under the following conditions: (a) in H_2O as solvent at 0.297 T; (b) in H_2O as solvent at 0.320 T; and (c) in D_2O as solvent at 0.320 T. Other conditions include the following: microwave power, 2.0 mW; frequency, 9.56 GHz; temperature, 8.0 K; sweep time, 42 s; FM amplitude, 200 kHz; RF power, 400 W (nominal).

$A_\parallel$ pointing toward the vanadium, approximately along the V=O bond. For coordination to an equatorial VO^{2+} position, the protons should have $|A_\parallel| = 9$–18 and $|A_\perp| = 0$–5 MHz, and the tensor should be oriented with $A_\parallel$ pointing toward the vanadium and perpendicular to the V=O bond.

The ENDOR spectrum of Figure 6a was taken at the $-5/2_\parallel$ feature of the EPR spectrum (Figure 3a, feature A), so that the major contribution to the EPR (and hence the ENDOR) intensity at this field position is from molecules with the field oriented along the V=O bond. This orientation selection limits the possible proton superhyperfine couplings strictly on geometrical grounds, so that only superhyperfine tensor components directed along the z-axis (the V=O bond direction) will be detected. Thus, only the $|A_\perp| = 0$–5 MHz from equatorial coordination or $|A_\parallel| = 6.5$ MHz from axial coordination of the ligand can be observed with this orientation selection. Consequently, the small 2.2-MHz coupling observed in the ENDOR spectrum of Figure 6a,b can arise only from the equatorial coordination of water or an RNH_2 group.

DISCUSSION

VO^{2+} Can Substitute Functionally for Mg^{2+} in Isolated CF_1. Purified CF_1 has been shown to use a variety of metals as cofactors for ATP hydrolysis, including Mg^{2+}, Ca^{2+}, Mn^{2+}, and Cr^{3+}, by coordinating the phosphate oxygens (Vambutas & Racker, 1965; Hochman & Carmeli, 1981; Frasch & Selman, 1982). However, free metal is a competitive inhibitor of the ATPase reaction. The metal-binding affinity to CF_1 has been correlated with the ability both to activate and to inhibit ATPase activity (Hochman & Carmeli, 1981). The effects of VO^{2+} as a cofactor and inhibitor of ATPase activity generally conform to this relationship, such that the apparent

K_M is lower with VO^{2+} than with Ca^{2+} at limiting free metal, but Ca^{2+} is more effective as a cofactor when the free metal concentration becomes sigificant.

When VO^{2+} is used as a cofactor, the extent of inhibition induced by free ATP is diminished significantly compared to Ca^{2+} or Mg^{2+}. This inhibition is modulated to a greater extent when the metals at the catalytic sites differ from that loaded into the noncatalytic N2 site (Figure 2). These data show that while VO^{2+} used at the catalytic site decreased the inhibition apparently induced by free ATP, it had the opposite effect when specifically bound to one of the noncatalytic sites. Recent studies indicate that ATPase activity is modulated by the ATP or by Mg^{2+}-dependent binding of pyrophosphate to the noncatalytic sites (Jault & Allison, 1993). The results presented here indicate that metal bound to at least one of these sites significantly contributes to the observed modulations.

Coupling of Nitrogen to Vanadyl Probably Results from Coordination by a Lysine Amine. The presence of nitrogen in the coordination sphere of the metal is indicated by the strong isotropic superhyperfine coupling of 5.0 MHz derived from the ESEEM data of Figure 5. The coupling of VO^{2+} to coordinated nitrogen in various forms has been measured in studies of VO^{2+} model complexes, as well as when bound to specific sites of enzymes that have either histidine or lysine ligands. As summarized in Table 2, coordination of VO^{2+} by histidine typically results in an A_0 for a ligated ^{14}N of 6.3–7.5 MHz as opposed to a range of 4.0–5.6 MHz for lysine ligands. The nonligated ^{14}N of a histidine ligand has been determined to have a coupling constant 20-fold lower (Dikanov et al., 1993). The observed coupling of 5.0 MHz suggests that the VO^{2+} bound to CF_1 reported here has a lysine ligand. Although the amine group from the N-terminus of one of the subunits cannot be ruled out, the coordinated nitrogen reported here is remarkably similar to the metal-binding site of *S*-adenosylmethionine (AdoMet) synthetase, for which lysine ligation has been shown conclusively using ^{15}N labeling (Zhang et al., 1993). Like CF_1, the lysine at the AdoMet synthetase-binding site shows a coupling of about 5.0 MHz that is also isotropic.

The Most Probable Set of Equatorial Ligands for VO^{2+}. Table 2 also compares the ^{51}V hyperfine couplings observed for VO^{2+} bound to CF_1 obtained from the cw-EPR spectrum of Figure 3 to those of VO^{2+} bound to other enzymes. The **g** and **A** tensors have been shown to reflect the nature of the equatorial ligands, such that the ^{51}V hyperfine coupling decreases in order with the following ligands to VO^{2+}: H_2O > $RCOO^-$ = $RH_2PO_3^-$ > R=NR′ > RNH_2 > RO^- > RSH (Chasteen, 1981; Holyk, 1979; Markham, 1984). These studies also determined that the ^{51}V hyperfine coupling for VO^{2+} with a mixed ligand environment can be estimated by averaging the couplings found for the complexes with just one type of ligand and weighting the average by the number of each type. The additivity relation for the parallel hyperfine coupling takes the form

$$A_{\parallel \mathrm{calc}} = \sum n_i A_{\parallel i}/4 \qquad (4)$$

where i denotes the different types of equatorial ligand donor groups, n_i (= 1–4) is the number of ligands of type i, and $A_{\parallel i}$ is the measured coupling constant (from model studies) when all four equatorial ligand donor groups are of type i (Chasteen, 1981).

The ESEEM results presented here indicate at least one nitrogen ligand to the bound VO^{2+}. Previous studies of Mn^{2+} bound to CF_1 under the same conditions used to bind VO^{2+} here indicated the presence of a single water molecule coordinated to the metal (Haddy et al., 1989). These results are consistent with the ENDOR experiments reported here that show that water and/or nitrogen are equatorial ligands. Table 2 also contains the couplings expected for a few ligand combinations calculated from eq 4 using the published ^{51}V hyperfine couplings for uniform ligand environments. If we assume equatorial coordination by nitrogen and water, the best fit of the spin-Hamiltonian parameters from the data of Figure 3 is obtained when one nitrogen (probably lysine), two carboxyl oxygens (glutamate or aspartate), and one water compose the equatorial ligands for the VO^{2+} bound to CF_1, as shown in Figure 7. The observed hyperfine couplings place an upper limit of one on the number of equatorially bound nitrogens.

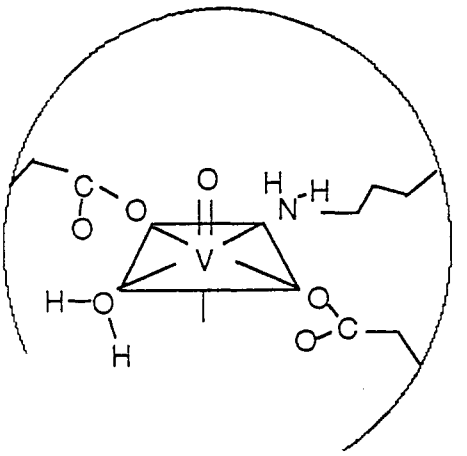

FIGURE 7: Equatorial ligands to the VO^{2+} bound to latent CF_1 depleted of metals and nucleotides from all but the N1 site, as derived from the additivity relationship. This is the best fit to the site that contains coordinated lysine.

The CF_1 used for the binding studies presented here was depleted of metals and nucleotides from all but the M1 and N1 sites, respectively. Due to the facts that the N2 site would be the depleted site with the greatest affinity and that nucleotide binding to this site is strictly metal-dependent, it is likely that the M2 metal-binding site described in Figure 7 is the N2 site in the absence of nucleotide.

As shown in Figure 4, CF_1 binds VO^{2+} in a strongly cooperative manner to the M2 and M3 sites, as previously observed for Mn^{2+} (Haddy et al., 1985; Hochman & Carmeli, 1985). The cw-EPR spectrum of Figure 3 suggests that the VO^{2+} has bound to a single type of site. Since the N2 site is believed to be noncatalytic, this would imply that the M2 and M3 sites were both noncatalytic. However, attribution of both cooperative metal sites to noncatalytic sites is inconsistent with the order of filling of nucleotides in CF_1, where evidence suggests that both the N3 and N4 sites are catalytic such that the next noncatalytic site to fill is N5 (Bruist & Hammes, 1981; Shapiro & McCarty, 1991). A good fit to the data derived from Figure 3 is also obtained from the additivity relation using one serine, one carboxyl oxygen, and two waters as equatorial ligands (Table 2, last row). Alternatively, it is possible that M2 and M3 are the metal-binding sites associated to the N2 and N3 nucleotide sites, respectively, of which only one metal site contains the nitrogen ligand visible by ESEEM. The observation that nucleotide binding to the N3 site does not have a strict metal requirement is explained if its associated metal site is previously filled by the cooperative binding of metals to M2 and M3 upon filling the N2 site.

ADDED IN PROOF

Due to misleading information provided by the supplier concerning the degree of hydration of $VOSO_4$ and, thus, the formula weight, the ratios of VO:ATP in Figure 1 should read 0.33:1 (a), 0.67:1 (b), and 1:1 (c) and in Figure 2 0.67:1. However, the qualitative conclusions from these experiments remain unchanged.

ACKNOWLEDGMENT

The authors thank Alex Gray and Alyson Roskelley for excellent technical support.

REFERENCES

Abragam, A., & Bleaney, B. (1970) in *Electron Paramagnetic Resonance of Transition Ions*, Oxford University Press, Oxford, U.K.

Albanese, N. F., & Chasteen, N. D. (1978a) *J. Phys. Chem. 82*, 910–914.

Albanese, N. F., & Chasteen, N. D. (1978b) *J. Phys. Chem. 82*, 2758.

Atherton, N. M., & Shackleton, J. F. (1980) *Mol. Phys. 39*, 1471–1485.

Böttcher, R., Heinhold, D., & Windsch, W. (1979) *Chem. Phys. Lett. 65*, 452–455.

Bruist, M. F., & Hammes, G. G. (1981) *Biochemistry 20*, 6298–6305.

Carmeli, C., Huang, J., Mills, D., Jagendorf, A., & Lewis, A. (1986) *J. Biol. Chem. 261*, 14171–14177.

Chasteen, N. D. (1981) in *Biological Magnetic Resonance* (Berliner, L., & Reuben, J., Eds.) pp 53–119, Plenum, New York.

Chen, P. S., Toribara, T. Y., & Warner, H. (1956) *Anal. Chem. 28*, 1756–1758.

Cross, R. L., & Nalin, C. M. (1982) *J. Biol. Chem. 257*, 2874–2881.

DeKoch, R. J., West, D. J., Cannon, J. C., & Chasteen, N. D. (1974) *Biochemistry 13*, 4347–4354.

Dikanov, S. A., Burgard, C., & Hüttermann, J. (1993) *Chem. Phys. Lett. 212*, 493–498.

Eaton, S. S., & Eaton, G. R. (1990) in *Vanadium in Biological Systems* (Chasteen, N. D., Ed.) pp 199–222, Kluwer Academic Publishers, Dordrecht, The Netherlands.

Eaton, S. S., Dubach, J., More, K. M., Eaton, G. R., Thurman, G., & Ambruso, D. R. (1989) *J. Biol. Chem. 264*, 4776–4782.

Frasch, W. D., & Selman, B. R. (1982) *Biochemistry 21*, 3636–3643.

Froncisz, W., & Hyde, J. S. (1980) *J. Chem. Phys. 73*, 3123–3131.

Gerfen, G. J., Hanna, P. M., Chasteen, N. D., & Singel, D. J. (1991) *J. Am. Chem. Soc. 113*, 9513–9519.

Girault, G., Berger, G., Galmiche, J.-M., & Andre, F. (1988) *J. Biol. Chem. 263*, 14690–14695.

Guerrero, K. J., Xue, Z., & Boyer, P. D. (1990) *J. Biol. Chem. 265*, 16280–16287.

Haddy, A. E., Frasch, W. D., & Sharp, R. R. (1985) *Biochemistry 24*, 7926–7930.

Haddy, A. E., Frasch, W. D., & Sharp, R. R. (1989) *Biochemistry 28*, 3664–3669.

Hanna, P. M., Chasteen, N. D., Rottman, G. A., & Aisen, P. (1991) *Biochemistry 30*, 9210–9216.

Hiller, R., & Carmeli, C. (1985) *J. Biol. Chem. 260*, 1614–1617.

Hochman, Y., & Carmeli, H. (1981) *Biochemistry 20*, 6287–6292.

Holyk, N. (1979) M.S. Thesis, University of New Hampshire, Durham, NH.

Jault, J.-M., & Allison, W. S. (1993) *J. Biol. Chem. 268*, 1558–1566.

Kirste, B., & van Willigen, H. (1982) *J. Phys. Chem. 86*, 2743–2749.

Leckband, D., & Hammes, G. G. (1987) *Biochemistry 26*, 2306–2312.

LoBrutto, R., Smithers, G. W., Reed, G. H., Orme-Johnson, W., Tan, S. L., & Leigh, J. S. (1986) *Biochemistry 25*, 5654–5660.

Lord, K., & Reed, G. H. (1990) *Arch. Biochem. Biophys. 281*, 124–131.

Markham, G. D. (1984) *Biochemistry 23*, 471–478.

Maurice, A. M. (1980) Ph.D. Thesis, University of Illinois, Urbana, IL.

Moroney, J. V., Lopresti, L., McEwen, B. F., McCarty, R. E., & Hammes, G. G. (1983) *FEBS Lett. 158*, 58–62.

Mulks, C. F., Kirste, B., & van Willigen, H. (1982) *J. Am. Chem. Soc. 104*, 5906–5911.

Murataliev, M. B. (1992) *Biochemistry 31*, 12885–12892.

Murataliev, M. B., Milgrom, Y. M., & Boyer, P. D. (1991) *Biochemistry 30*, 8305–8310.

Mustafi, D., Telser, J., & Makinen, M. W. (1992) *J. Am. Chem. Soc. 114*, 6219–6226.

Nilges, M. J. (1979) Ph.D. Thesis, University of Illinois, Urbana, IL.

Reijerse, E. J., Shane, J., de Boer, E., & Collison, D. (1989) in *Electron Magnetic Resonance of Disordered Systems* (Yordanov, N. D., Ed.) pp 189–204, World Scientific Publishers, Singapore.

Shapiro, A. B., Huber, A. H., & McCarty, R. E. (1991) *J. Biol. Chem. 266*, 4194–4200.

Tipton, P. A., McCracken, J., Cornelius, J. B., & Peisach, J. (1989) *Biochemistry 28*, 5720–5728.

Weil, J. A., & Hecht, A. G. (1963) *J. Chem. Phys. 38*, 281–286.

White, L. W., & Chasteen, N. D. (1979) *J. Phys. Chem. 83*, 279–284.

Xue, Z., Zhou, J.-M., Melese, T., Cross, R. L., & Boyer, P. D.(1987) *Biochemistry 26*, 3749–3753.

Zhang, C., Markham, G. D., & LoBrutto, R. (1993) *Biochemistry 32*, 9866–9873.